J. Fluid Mech. (2002), *vol.* 452, *pp.* 25–37.
DOI: 10.1017/10.1017/S0022112001006541 Printed in the United Kingdom

Salt fingers at low Rayleigh numbers

By R. KRISHNAMURTI, Y.-H. JO† AND A. STOCCHINO‡

Department of Oceanography and Geophysical Fluid Dynamics Institute, Florida State University, Tallahassee, FL 32306, USA

(Received 9 March 2001 and in revised form 1 August 2001)

This is a laboratory study of salt fingers at low Rayleigh numbers. We report on the stability boundary in the (R_S, R_T)-plane (where R_S and R_T are the salt and heat Rayleigh numbers respectively), the wavenumber of the observed fingers, and the planform. In this low R_S, R_T range, fingers have width comparable to their height, as predicted by linear stability theory. The planform appears to be close-packed polygonal cells when they are formed on curved profiles of temperature and salinity. However, the planform is distinctly rolls when care is taken to approximate linear profiles.

1. Introduction

When the density, ρ, of a fluid is determined by two components such as temperature (T) and salinity (S), which diffuse at different rates, flows can occur even when the fluid is statically stably stratified. Furthermore, when the fast diffuser (temperature) is stabilizing (hot above, cold below) and the slow diffuser is destabilizing (salty above, fresh below) in such a way that the density decreases upwards, salt fingers can grow as an instability. Initially hot salty fluid can sink if its excess temperature can be diffused away to a cooler environment while it retains its excess salinity. This can occur only because the diffusivity of salt in water is much smaller than the diffusivity of heat.

Salt fingers in laboratory experiments are most often seen as a close-packed array of tall and narrow flow structures. In a laboratory tank 2 m in height, fingers can be seen which are vertically coherent for the full 2 m extent, while the horizontal dimension of each finger is no more than several millimetres. Part of such a 2 m tall shadowgraph is shown in figure 1. This horizontal scale has been shown (Stern 1969) to be of order $R_T^{-1/4}$, where the Rayleigh number R_T is defined below. Laboratory observations (Shirtcliffe & Turner 1970; Linden 1973) confirm this scaling. In fact, our 2 m tall fingers with 3 mm width fit directly on an extrapolation of their quarter-power curve. The horizontal planform of such tall fingers has also been observed by Shirtcliffe & Turner (1970). In an evolving finger interface, where the fingers between two reservoirs grow in height, they show that when the fingers are 4.5 cm tall (Rayleigh number $R \approx 10^8$) the planform shows distinctly square structures.

On the other hand, we recall that the linear stability theory of Baines & Gill (1967) predicts short, 'fat' fingers, of width comparable to their height, at least at low Rayleigh numbers. In figure 2(a), for example, the curve labelled E is that on which

† Present address: University of Delaware.
‡ On leave from the University of Genoa, Italy.

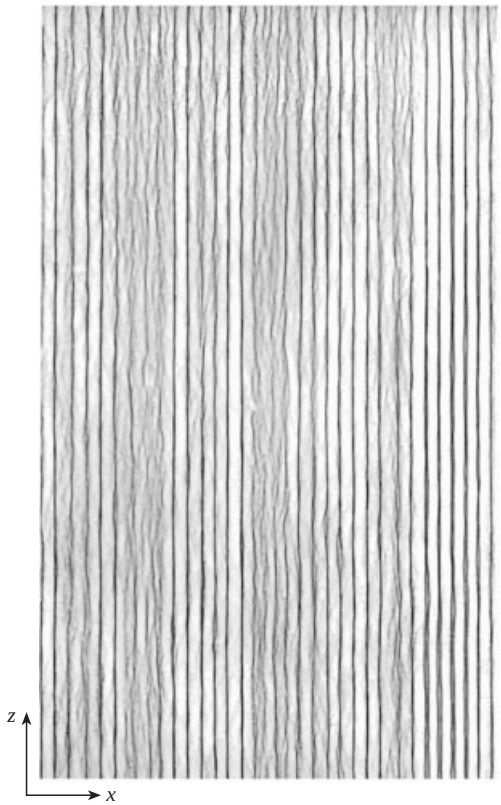

FIGURE 1. Tall, slender salt fingers at $R_S = 0.81 \times 10^{16}$, $R_T = 1.1 \times 10^{16}$. This figure shows a 20 cm tall section taken from a shadowgraph showing 2 m tall salt fingers. Most of the fingers were vertically coherent. Their average horizontal size was 3.4 mm.

fingers with horizontal wavenumber $\alpha = 1$ have maximum growth rate. These fingers are as wide as they are tall. Such fat fingers have never been reported as a laboratory observation. It is easy to see why this would be the case. We often use salt as a proxy for cold and sugar as a proxy for salt in order to drive salt fingers. The diffusivity of salt in water is $\kappa_T \simeq 10^{-5}\,\mathrm{cm^2\,s^{-1}}$, that of sugar in water is $\kappa_S \simeq 0.3 \times 10^{-5}\,\mathrm{cm^2\,s^{-1}}$. For dilute solutions the kinematic viscosity ν is near that for pure water, that is, $\nu \simeq 10^{-2}\,\mathrm{cm^2\,s^{-1}}$. We can estimate the conditions necessary in order to attain thermal Rayleigh number R_T and salt Rayleigh number R_S of order 10^3, where R_T and R_S are defined as

$$R_T = g\beta_T \Delta T d^3/\kappa_T \nu,$$

$$R_S = g\beta_S \Delta S d^3/\kappa_T \nu.$$

Here g is the acceleration due to gravity, β_T the thermal expansion coefficient, β_S the salt 'expansion' coefficient, d the layer depth, and ΔT the temperature excess, ΔS the salinity excess, at the top boundary over that of the bottom boundary. A reasonably small but measurable value of $\beta_T \Delta T$ or $\beta_S \Delta S$ might be 10^{-3}. Then to attain $R_T, R_S \simeq 10^3$ would require depth d of approximately 0.5 mm. So it is not surprising that this region of the R_T, R_S parameter space is rarely observed.

We see further from figure 2(a), or the equivalent log-log plot of figure 2(b), that 'fat' fingers, having a horizontal wavenumber $\alpha \simeq 1.0$, have maximum growth rate

not only at $R_T, R_S \simeq 10^3$ but that the curve of $\alpha = 1.0$ extends to larger R_T, R_S. Implicit in this discussion is the assumption that maximum growth rate from linear theory implies realization in an experiment. Of course the validity of this assumption is not proven. Even if valid, there is the further difficulty that as R_T and R_S are increased, the $\alpha = 1$ curve and the higher α curves all approach the stability boundary $R_T = (27/4)\pi^4 + R_S/\tau$. This is illustrated in figure 2(*c*), where we have plotted the R_S-separation between various curves as $|R_T|$ is increased, showing that the curves for $\alpha^2 = 1$ and $\alpha^2 = 1.2$ which were widely separated at $|R_T| \simeq 10^3$, have nearly merged at $|R_T| \simeq 10^7$. Experimentally, this means that unrealistically fine precision in setting R_T and R_S would be required in order to place the state of the system near the curve of $\alpha^2 = 1$ rather than the curve of $\alpha^2 = 50$. At $R_T = 10^7$, an error of 0.1% in R_S may place us in the stable range (no fingers) or in the range of very narrow ($\alpha^2 = 50$) fingers.

In the experiments reported here we have chosen to investigate fingers at low R_T, R_S. By adding methyl cellulose to water we have produced a fluid whose viscosity can be increased by several orders of magnitude over that of pure water. The salt or sugar diffusivity in this fluid is shown to be relatively little changed from that in water, so that the product $\kappa\nu$ is increased and R_T, R_S are decreased.

The linear stability theory gives the overall wavenumber α with maximum growth rate, but does not determine the partitioning of α^2 into horizontal components α_x^2 and α_y^2, that is, it cannot select planform. We have not done the finite-amplitude calculation and the investigation of the stability of the finite-amplitude flows. Rather we rely on past experience with Rayleigh–Bénard convection where we have learned that a linear profile of temperature and constant values of material coefficients leads to rolls as the only stable finite-amplitude solution (Schluter, Lortz & Busse 1965), whereas a curved temperature profile can lead to stable hexagonal flows for a finite range of parameters (Krishnamurti 1968*a*, *b*). Indeed we will show that salt fingers have a roll planform for a nearly linear profile of T and S, while the planform shows polygonal cells with curved profiles of T and S.

We also report on the observed finger size and stability boundary for sugar/salt fingers in a Hele-Shaw cell in which the critical Rayleigh number is increased by the closeness of the sidewalls. The minimum Rayleigh number for onset of stationary salt fingers in a Hele-Shaw cell is attained at wavenumber $\alpha^2 = 1$, giving

$$r_{T\,min} = \frac{r_S}{\tau} + 4\pi^2,$$

where

$$r_T = \left(\frac{g\beta_T \Delta T d^3}{\kappa_T \nu}\right)\left(\frac{b^2}{12d^2}\right) = \frac{b^2}{12d^2} R_T,$$

$$r_S = \left(\frac{g\beta_S \Delta S d^3}{\kappa_T \nu}\right)\left(\frac{b^2}{12d^2}\right) = \frac{b^2}{12d^2} R_S,$$

and where b is the gap between the two sidewalls.

2. Experimental procedure

2.1. *High-viscosity experiments*

The high-viscosity fluids were methyl cellulose in water, or glycerol in water. The methyl cellulose solution was produced by dissolving 100 g of methyl cellulose in 1 l of distilled water. A Rheoscopic tracer was added to this solution. This stock solution

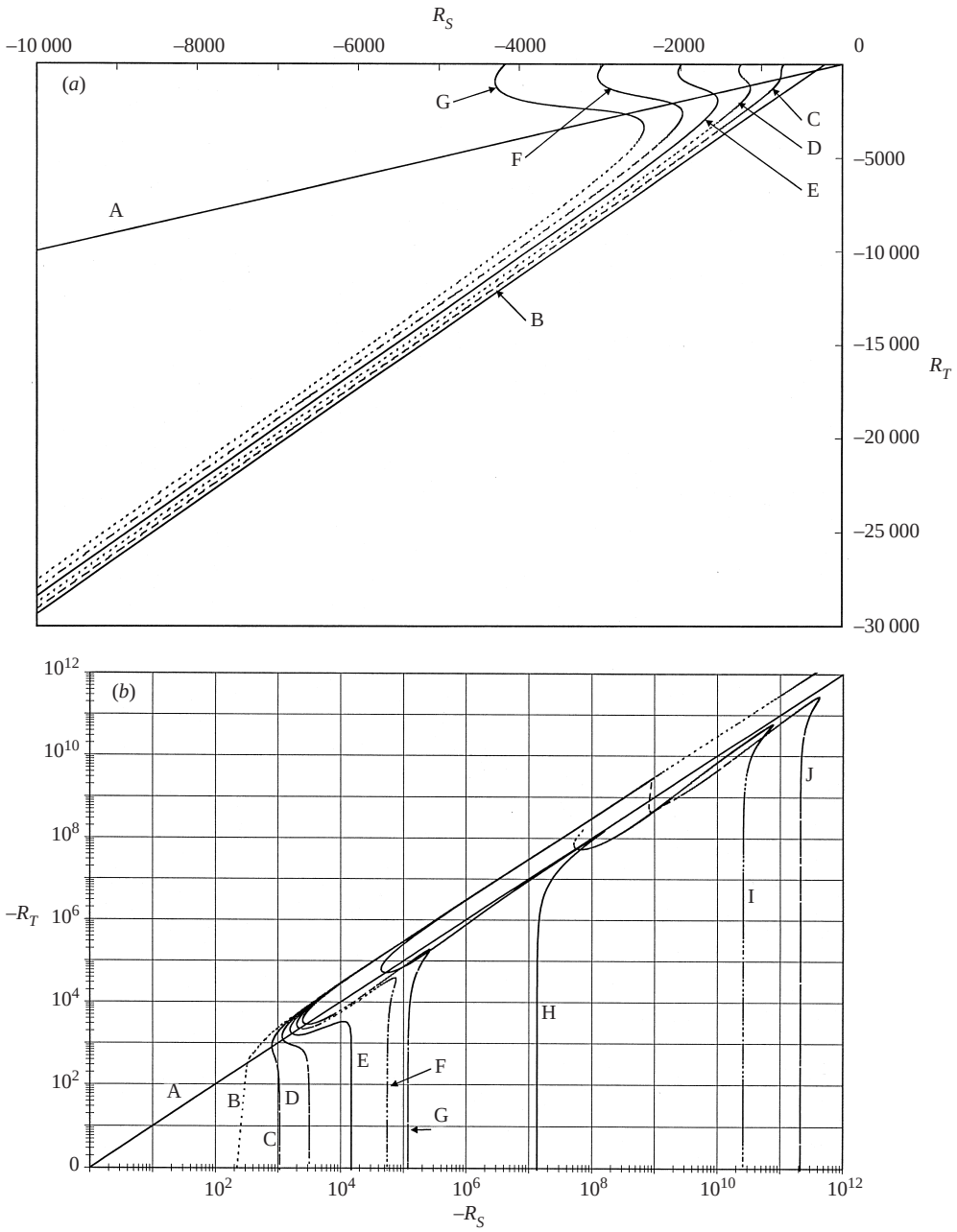

FIGURE 2. For caption see facing page.

was diluted with varying volumes of water to produce fluids with viscosities ranging from 20 cP to 700 cP. Viscosities were measured using a Haake falling ball viscometer.

These experiments were conducted in several different tanks: a circular glass cylinder 19 cm in diameter with variable depth; a rectangular tank of horizontal dimension 9 cm by 18 cm with variable depth; circular cylinders of diameter 10 cm.

Two classes of high-viscosity experiments were performed. The first will be called the curved profile experiments; the second will be called the linear profile experiments.

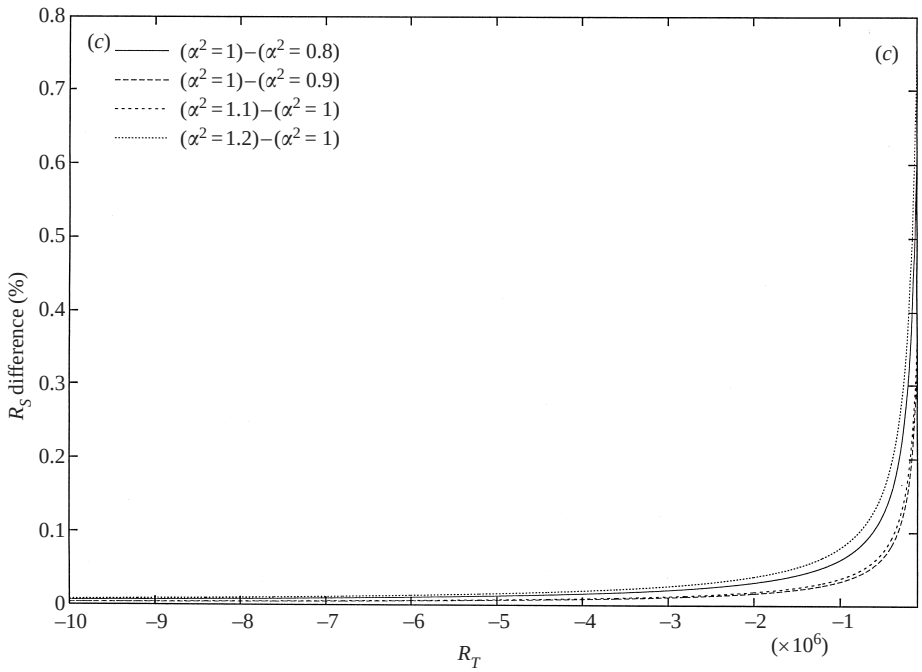

FIGURE 2. (*a*) The salt finger stability diagram (after Baines & Gill 1969) showing lines of constant squared wavenumber α^2 for the most unstable mode. This is like their figure 5, except that here the diffusivity ratio $\tau = 1/3$, Prandtl number $\sigma = \nu/\kappa_T = 10^3$. The labelling of the curves is as follows: A: $R_T = R_S$, B: marginal stability boundary, C: $\alpha^2 = 0.8$, D: $\alpha^2 = 0.9$, E: $\alpha^2 = 1.0$, F: $\alpha^2 = 1.1$, G: $\alpha^2 = 1.2$. There is no significance to the patterns that form the lines; the dots/dashes/solid lines are purely for ease in distinguishing one line from another. (*b*) As in (*a*), except that the log-log plot allows display of a greater range of α^2, up to $\alpha^2 = 100$. The labeling of the curves is as follows: A: $R_T = R_S$, B: marginal stability boundary, C: $\alpha^2 = 0.8$, D: $\alpha^2 = 0.9$, E: $\alpha^2 = 1.0$, F: $\alpha^2 = 1.1$, G: $\alpha^2 = 1.2$, H: $\alpha^2 = 4$, I: $\alpha^2 = 50$, J: $\alpha^2 = 100$. (*c*) Percent separation in R_S of the curves of (*a*) as it varies with R_T, showing the convergence of the curves of constant α^2 as R_T is increased.

In the first, a tightly stretched horizontal porous membrane of Versapor 800 filter (see the Appendix for details) separated two fluids initially identical except that the lower fluid contained salt and was more dense by $\Delta\rho$ than the upper fluid, which contained sugar. With time, salt from the lower layer diffuses through the membrane into the upper layer, and sugar from the upper layer diffuses (more slowly) into the lower layer. The profile of salinity is obtained by solving the diffusion equation for initial condition $S = 1$ in the lower layer, $S = 0$ in the upper layer; the boundary condition is no flux at the bottom of the lower layer, $z = -1$, and at the top of the upper layer, $z = 1$. The resulting curved salinity profile is shown in figure 3(*a*) at time $\tau_{1/2}/\pi^2$, where $\tau_{1/2} = d_{1/2}^2/\kappa_T$ and $d_{1/2}$ is the upper layer depth. (When $d_{1/2} = 1$ cm, $\tau_{1/2} \simeq 1$ day.)

A typical example may be 10 g NaCl dissolved in 50 ml of distilled water, added to 500 ml of methyl cellulose stock solution for the lower layer; 6 g sucrose dissolved in 50 ml distilled water added to 500 ml of identical methyl cellulose stock solution for the upper layer. Many experiments were also conducted using glycerol in water instead of methyl cellulose in water. A clear Plexiglas lid was placed over the top, in contact with the fluid, to prevent Marangoni convection.

In the second class of high-viscosity experiment, we used no porous membranes,

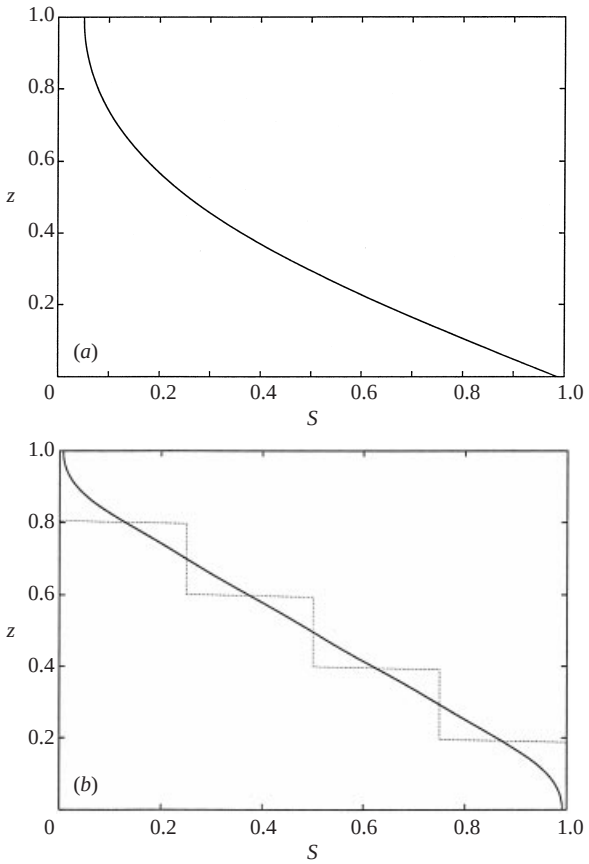

FIGURE 3. (*a*) Curved vertical profile of salinity S in the upper layer above the porous membrane, at one diffusion time. The diffusion equation was solved for initial condition $S = 0$ at $1 \geqslant z > 0$, $S = 1$ at $0 > z \geqslant -1$. The boundary condition was $S_z = 0$ at $z = 1, -1$. The solution is shown at time $t = 1/40$ which is approximately $\tau_{1/2}/\pi^2$, where $\tau_{1/2}$ is the diffusion time for the half-layer; t is non-dimensionalized by the diffusion time for the full layer. (*b*) Nearly linear vertical profile of salinity (solid line) from an initially discretized five-layer state (dotted line). See text. The diffusion equation was solved for intial salinity shown by the dotted line, and boundary condition $S_z = 0$ at $z = 0, 1$. The solution is shown at time $t = 1/250$ which is approximately $\tau_{1/5}/\pi^2$, where $\tau_{1/5}$ is the diffusion time for depth 0.2; t is non-dimensionalized by the diffusion time for the full layer.

but attempted to make nearly linear profiles of sugar and salt by a discretized two-bucket method, laying down layer by layer a discretized version of the desired linear gradients. Thus, we may take the two solutions of the typical example described above, and place the salty solution to a depth of 2 mm in the bottom of the 9 cm by 18 cm rectangular tank. If the total desired depth was 6 mm, the next 2 mm layer was a mixture of 50% salty solution and 50% sugar solution. The top layer was totally sugar solution. In order to make 2 mm layers of uniform depth, a screen on a float was used. The screen was 8.8 cm by 17.8 cm and was made of several layers of tulle fabric and a layer of metal window screen mesh for rigidity. These were attached to a Styrofoam float, so constructed that only 1 cm width around the perimeter of the screen was blocking fluid passage. The screen allowed successive additions of 2 mm depth to slowly ooze down to form the next fluid layer, while the Styrofoam kept the screen afloat with little disruption to the layer below. The success of this procedure

was tested by colour-coding each layer and checking visually for uniformity of depth. The diffusion time across a depth of 2 mm was 4×10^3 s. The computed profile in a five-layered fluid after time $\tau_{1/5}/\pi^2$, where $\tau_{1/5}$ is the diffusion time $(d/5)^2/\kappa_S$ for one-fifth of the layer, is shown in figure 3(*b*). It might be argued that this is closer to a linear profile than is figure 3(*a*).

The diffusivity of NaCl in the methyl cellulose solution was determined as follows. The conductivity probe used was in the shape of a hollow cylinder open at both ends. It is 15 cm long, with outside diameter 1.0 cm, inside diameter 0.5 cm. Extended-area electrodes are built into this inner cylindrical surface. The salty fluid was prepared as described above and placed in the bottom of the container. A stretched Versapor 800 membrane separated this salty fluid from the initially salt-free fluid placed above the membrane. The conductivity probe was placed vertically in the upper fluid so that the bottom opening was 1.0 cm above the membrane. The probe was immersed to a depth of 3.0 cm of upper layer fluid. It was kept in this position for the duration of the measurement. It was expected that the 0.5 cm diameter by 3.0 cm tall volume of fluid initially trapped in this probe would gradually become more conductive as salt diffused upwards into it. The time history of the measured salinity was recorded and compared with the resulting curves produced with identical geometry when salt diffused in water free of methyl cellulose. It was not difficult to extend the zero salinity part of the curve to intersect with the increasing salinity part of the curve to define an intersection time t_I. By taking the ratio of t_I for salt diffusing in methyl cellulose solution to that for diffusion in water, we effectively eliminate the undefined distance from the membrane boundary to the electrode. The ratio of the intersection times then gives the ratio of the diffusivities. This comparison method was used because the large surface of the electrodes in the probe would not allow determination of conductivity at a point as a function of time. As salt diffuses upward into the fluid trapped in the probe, the conductivity reading increases in part because of the increasing salinity at a single point, but also in part because of salt reaching other points on the extended electrode. A micro-probe was not used since it cannot be expected to give long-term stable readings. We did not have access to a stable quadruple micro-probe of the kind designed by Head (1983).

Measurement of diffusivity of sugar in methyl cellulose solution was attempted with sugar solution below the Versapor 800 filter and initially sugar-free solution above. The optical rotation by sugar was used. Great precision could not be attained because the laser beam was scattered and attenuated in a short distance through the methyl cellulose.

2.2. *Hele-Shaw cell experiments*

These experiments were conducted in a container made with glass plates which formed the vertical walls of the tank. The spacing between the plates was 0.10 cm. Fluid filled this tank to a depth of either 0.40 cm or 0.80 cm. The fluid used was water containing sugar for the slow diffuser and salt for the fast diffuser.

Huppert & Manins (1973) showed that, for the case of an initially two-layer system, the stability boundary would have slope $\tau^{-3/2}$ rather than τ^{-1} as expected with linear gradients. Here τ is the ratio of the diffusivity of the slow diffuser (sugar) to that of the fast diffuser (salt). We attempted to approximate linear gradients in the Hele-Shaw cell experiments. The two-bucket method usually gives excellent linear gradients but in our case surface tension at the glass walls produced too large a disruption. In spite of careful cleaning of the glass surfaces, the two-bucket method produced horizontally non-uniform filling. The best results were obtained by carefully placing layer after

layer of fluid in the Hele-Shaw cell with a fine hypodermic needle and syringe. Fluid for each layer was prepared using a discretized version of the two-bucket method. Each layer laid down was approximately 2 mm in depth. Colour was used to indicate success in producing horizontally uniform gradients.

Chen & Sandford (1976) emphasized the importance of diffusion in destroying initially linear gradients when these are not maintained. In particular, salt diffusing upward faster than sugar diffusing downward tends to decrease the stabilization from below. Based on their experience, we placed a thin layer of finely powdered salt at the bottom of the Hele-Shaw cell and used a salt profile which started with saturated salt solution at the bottom. Above the working layer we placed an inert layer of pure water, which helps to maintain gradients at the top.

We visualized the flow in these experiments by adding a water-soluble liquid dye to one of the 2 mm deep layers, usually the top layer. Care was taken to measure the specific gravity of the fluids, including the dye, that were used in producing each layer. The specific gravity balance used allowed determination to 0.0001.

3. Observations

3.1. *High-viscosity experiments*

For most of the solutions tested, the ratio of the diffusivity of salt in the methyl cellulose solutions to its diffusivity in water was between 1.0 and 0.3, that is,

$$\kappa_T = 10^{-5}\,\mathrm{cm^2\,s^{-1}} \quad \text{to} \quad 3\times 10^{-6}\,\mathrm{cm^2\,s^{-1}},$$

while the viscosity was increased by factors of 10 to 10^2. Thus the characteristic time for salt to diffuse 1 cm is on the order of one day. The diffusivity of sugar in these solutions was found to be approximately

$$\kappa_S = 2\times 10^{-6}\,\mathrm{cm^2\,s^{-1}},$$

but because of the uncertainty in this measurement, we took the diffusivity ratio to be $1/3$ as in pure water.

3.1.1. *Curved profile experiments*

Approximately one hour after filling the apparatus with the two layers of fluid, a transient pattern of fine fingers with a horizontal scale of 1 mm or less is seen just above the membrane, in the bottom 1 or 2 mm of the upper layer which itself may be 1 cm deep. The plan view is one of a fine-scale uniform granulation. This lasts for several hours. One hour is the diffusion time for 2 mm.

After 10–20 hours (depending on the particular experiment), the flow in the fluid above the membrane is in the form of fat fingers whose width is comparable to the layer depth. Figures 4(*a*) and 5(*a*) show typical plan views of the fingers as seen from above. These flows have been made visible by rheoscopic tracers which show differential shear in the fluid. The numbers on the scale refer to centimetres. Figure 4(*a*) shows plan views of fingers in fluid 0.95 cm deep in the 10 cm diameter tank. Wavelengths non-dimensionalized by the depth range from 0.7 to 1.0, with corresponding α of 1.4 to 1.0. These flows last for 2 to 3 days. In their final decay they usually have the form of rolls of width comparable to the fluid depth (figure 4*b*). Figure 5(*a*) shows fingers in a fluid of depth 1.0 cm in the 9 cm by 18 cm tank. The quasi-periodic polygonal cells have spacing (measured from one bright region to the next) ranging from 0.7 cm to 1.0 cm. Using the layer depth to non-dimensionalize gives α ranging from 1.4 to 1.0. The Rayleigh numbers are $R_S = 8.6\times 10^4$, $R_T = 2.5\times 10^5$.

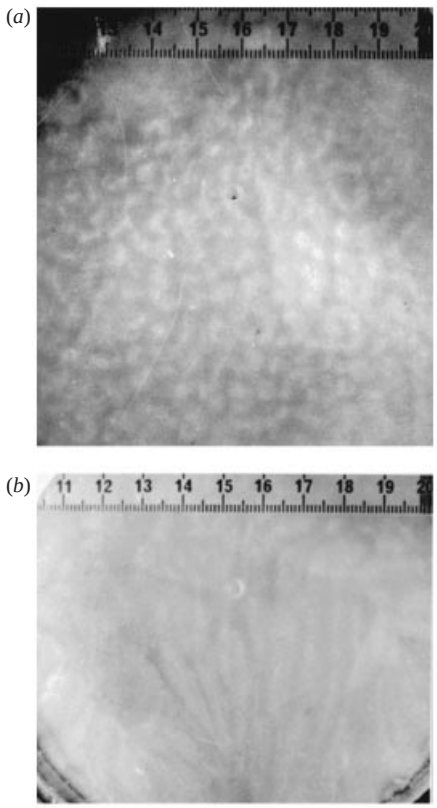

FIGURE 4. (*a*) Photograph showing a plan view of salt fingers at $|R_S| = 3.8 \times 10^4$, $|R_T| = 1.1 \times 10^5$. The fluid depth is 0.95 cm. The working fluid is methyl cellulose in water, viscosity 0.38 P. The diffusing components are sugar and salt. (*b*) After several days, the experiment in (*a*) has decayed to the roll-like structure shown here. The numbers on the scale are in cm.

3.1.2. *Linear profile experiments*

Approximately one hour after filling the three-layer discretization of linear profiles, the plan view is in the form of rolls of width comparable to the fluid depth (figure 5*b*). The various experiments are summarized in figure 6. The theoretical stability boundary $R_T \simeq R_S/\tau$ (neglecting R_c since $R_S/\tau \gg R_c \simeq 10^3$) on a log-log plot should have intercept $1/\tau$. The stability boundary, based on the observed stable points, is seen to have an intercept of 3.5.

3.2. *Hele-Shaw experiments*

These experiments are summarized in figure 7.

4. Discussion

Our high-viscosity experiments were conducted at $|R_T| \simeq 10^5$, $|R_S| \simeq 10^4$, $\sigma \simeq 10^5$, $\tau \simeq 1/3$. In terms of the energetics as computed by Baines & Gill, we have $B = -30$ where B, defined by their equation (4.2), is proportional to the ratio of terms in the energy equation. With large negative B our experiments are certainly in the range where energy is released from the salt (slow diffuser) gradient, and most of it is used to work against the temperature (fast diffuser) gradient. Also, at our large value of

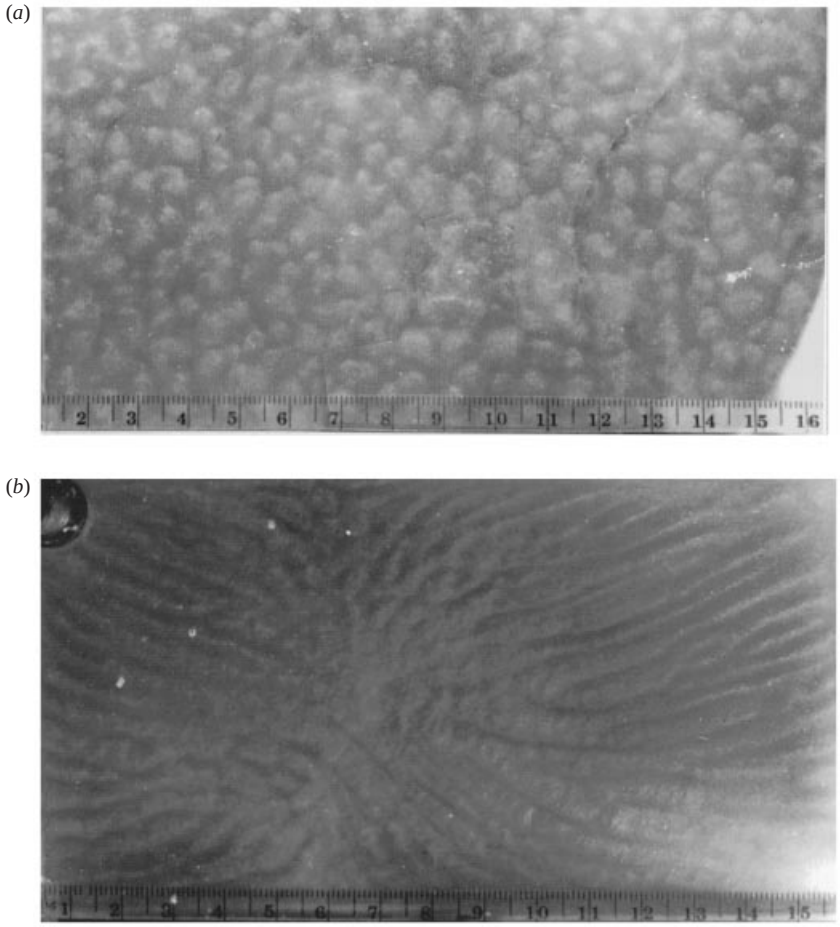

FIGURE 5. (*a*) Photograph showing a plan view of salt fingers at $|R_S| = 8.6 \times 10^4$, $|R_T| = 2.5 \times 10^5$ for curved profile of S and T. The fluid depth is 1.0 cm. The working fluid is methyl cellulose in water, viscosity 0.91 P. The diffusing components are sugar and salt. The numbers on the scale are cm. The dark shadows are reflections of camera and photographer on the Plexiglas lid of the tank. (*b*) Photograph showing a plan view of salt fingers at $|R_S| = 1.5 \times 10^4$, $|R_T| = 4.4 \times 10^4$ for linear profiles of T and S. The fluid depth is 0.6 cm, other parameters are as in (*a*).

σ, most of the energy remaining from these two effects is dissipated. Furthermore, referring to their figure 8, we see that our experiments are in a range where the time derivatives in the heat and vorticity equations can be neglected, as can the diffusion term in the slow-diffuser salt equation. In the fast-diffuser heat equation,

$$\frac{w\,\partial T}{\partial z} \sim \kappa_T \frac{\partial^2 T}{\partial x^2}$$

with $dz \sim dx \sim d$; the vertical advection time d/w is comparable to the lateral diffusion time d^2/κ_T. In other words, the Péclet number P_e is order unity:

$$P_e = \frac{w}{\alpha \kappa_T} = O(1).$$

Near onset, velocities may be slow enough that diffusion has time to act over horizontal distances comparable to the layer depth. Hot, salty parcels of width

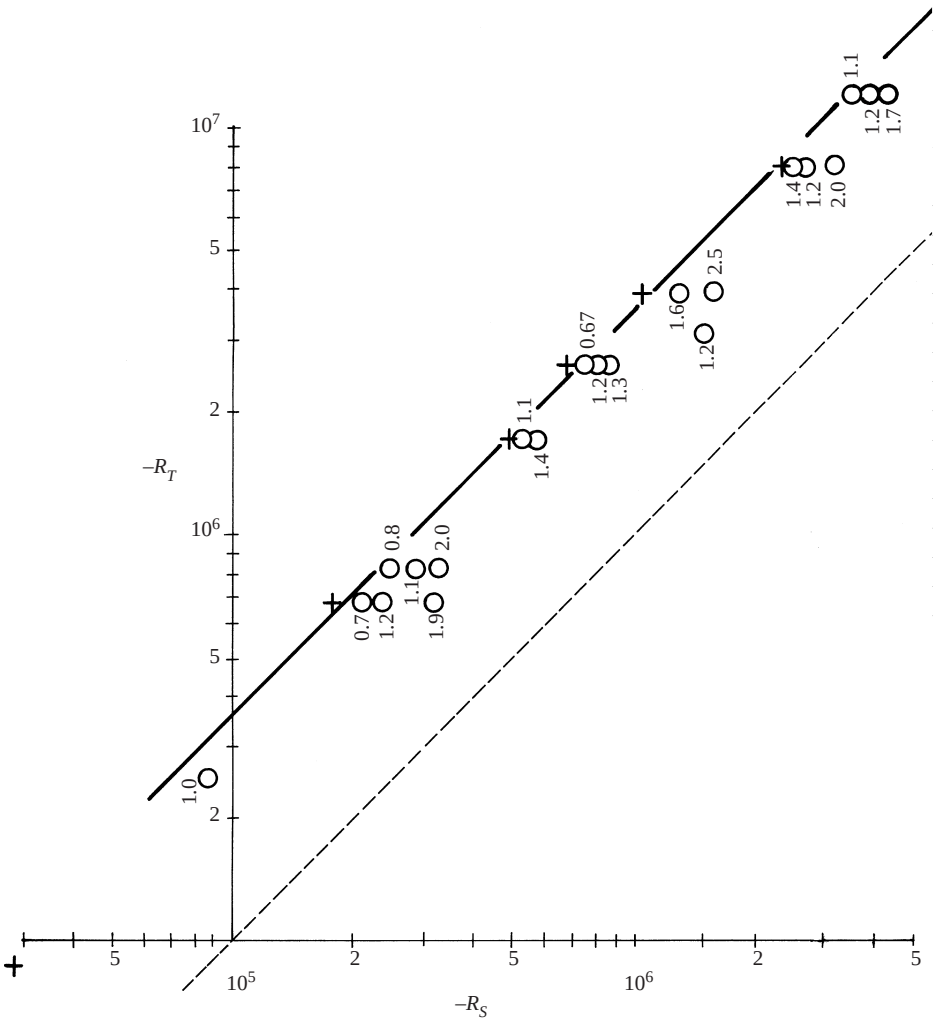

FIGURE 6. The salt finger stability diagram for high-viscosity fluids. The circles indicate the R_T, R_S at which fingers were observed. The numbers indicate the observed average wavenumber squared. The cross indicates a stability boundary where we observed no flow.

comparable to the layer depth may still sink (slowly) by diffusing away their excess temperature while retaining their salt, much as they would (at higher speed) in tall narrow fingers at higher Rayleigh numbers.

We have not attempted a precise determination of the stability boundary; this would best be done with flux measurements and application of the Schmit–Milverton principle (that is, extrapolating the conductive flux curve and the convective flux curve to the intersection point). Our observations are of finite-amplitude flows or of no flows, but no contradiction with theory was observed.

The observed planform of the fingers at R_S, R_T of order 10^4–10^5 was either polygonal cells for curved initial profiles, or rolls for near-linear profiles. This distinction between polygonal and roll cells was reproducible for the many (order 10) repetitions of the experiments. Squares were not observed in this parameter range with fat fingers, although Shirtcliffe & Turner (1970) clearly show squares with tall thin fingers at R_S, R_T

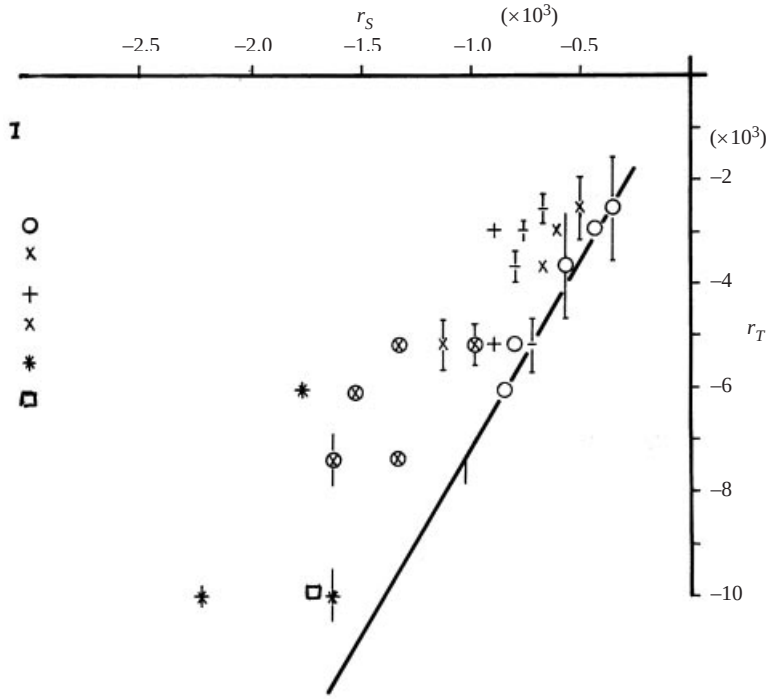

FIGURE 7. As in figure 6, except that the observations are for various Hele-Shaw cells (see text).

of order 10^8. The theory of Proctor & Holyer (1986), which predicts rolls, as well as that of Radko & Stern (2000), which predicts squares, apply specifically to tall thin fingers.

Crucial to these experiments was attaining low Rayleigh numbers by increasing viscosity, ν, while not appreciably decreasing the diffusivity, κ, of salt down its gradient. With a pure substance, the product $\nu\kappa$ might be expected from chemical theory to remain constant. However, with a binary fluid such as methyl cellulose dissolved in water, the large molecules of methyl cellulose determine the highly viscous behaviour in macroscopic fluid motion, but for diffusion on the molecular scale, small ions like Na and Cl can still diffuse through the H_2O part of the fluid, encountering large methyl cellulose polymers only occasionally (in a dilute solution).

Also crucial to these experiments is the use of a rigid lid on the methyl cellulose solution to prevent Marangoni convection. Flows were often observed in these solutions even in the absence of sugar or salt gradients, and such flows were always stopped by the placement of a rigid lid. Thermally driven cellular convection is ruled out, since a critical temperature difference of 10 °C must be exceeded for the 1 cm deep 1 P solution to convect and such large temperature differences were never encountered. In the case of the Hele-Shaw cells with smaller masses of water and conducting glass walls, we monitored the temperature difference between bottom and top of the fluid and never found a temperature difference even approaching critical.

5. Conclusions

At sufficiently low Rayleigh numbers salt fingers of width comparable to the fluid layer depth are observed. The observed finger width and stability boundary are in reasonable agreement with theory. The planform of these fingers, which is not

predicted by linear theory, was found to be polygonal cells for a curved profile and rolls for a linear profile of concentration.

This would have been a timely experimental result three decades ago. Nevertheless, even today it is the first laboratory confirmation of the linear stability theory which predicts that in the low Rayleigh number regime fingers as broad as they are tall should occur.

This research was supported in part by the National Science Foundation under grant number OCE-9809805. This is contribution number 415 of the Geophysical Fluid Dynamics Institute at Florida State University.

Versapor 800 is a commercially available filter which has pore size 0.8 micron and thickness 0.020 cm. We have used it extensively, stretching it under water onto a frame and holding it taut in an O-ring groove. Used in this way we have found that it allows diffusion of salt or sugar across it when there is a salt or sugar gradient applied. The pore size is such that diffusion is not inhibited by the filter but proceeds as normal diffusion down the gradient. Being stretched taut, the filter behaves as a rigid boundary to flow, in all our applications. Tests with thymol blue flow visualization showed no motion on one side of such a filter, while fluid on the other side of the filter was being constantly stirred with a magnetic stirring bar. Application of a pressure gradient across the filter can produce fluid flow through it, but of course we took care never to allow this. Clearly in our closed tanks such flow-through cannot occur. Some of these properties are given in Krishnamurti & Zhu (1989).

For the diffusion of sugar and salt in water we used the published values of Gosting & Morris (1949) and of Stokes (1950).

REFERENCES

Baines, P. G. & Gill, A. E. 1969 On thermohaline convection with linear gradients. *J. Fluid Mech.* **37**, 289–306.

Chen, C. F. & Sandford, R. D. 1976 Size and shapes of salt fingers near the marginal state. *J. Fluid Mech.* **78**, 601–607.

Gosting, L. J. & Morris, M. S. 1949 Diffusion studies on dilute aqueous sucrose solution at 1 and 25 °C with the Guoy interference method. *J. Am. Chem. Soc.* **71**, 1998–2006.

Head, M. J. 1983 The use of miniature four-electrode conductivity probes for high resolution measurement of turbulent density or temperature variations in salt-stratified water flows. PhD dissertation, University of California, San Diego.

Huppert, H. E. & Manins, P. C. 1973 Limiting conditions for salt fingering at an interface. *Deep-sea Res.* **4**, 553–560.

Krishnamurti, R. 1968*a* Finite amplitude convection with changing mean temperature. Part 1. Theory. *J. Fluid Mech.* **33**, 445–455.

Krishnamurti, R. 1968*b* Finite amplitude convection with changing mean temperature. Part 2. An experimental test of the theory. *J. Fluid Mech.* **33**, 457–463.

Krishnamurti, R. & Zhu, Y. 1989 Double diffusive convection with imposed vertical mass flux. *J. Mar. Res.* **48**, 1–21.

Linden, P. F. 1973 On the structure of salt fingers. *Deep-sea Res.* **20**, 325–340.

Proctor, M. R. E. & Holyer, J. Y. 1986 Planform selection in salt fingers. *J. Fluid Mech.* **168**, 244–253.

Radko, T. & Stern, M. E. 2000 Finite amplitude salt fingers in a vertically bounded layer. *J. Fluid Mech.* **425**, 133–160.

Schluter, A., Lortz, D. & Busse, F. 1965 On the stability of steady finite amplitude convection. *J. Fluid Mech.* **23**, 129–144.

Shirtcliffe, T. G. L. & Turner, J. S. 1970 Observations of the cell structure of salt fingers. *J. Fluid Mech.* **41**, 707–719.

Stern, M. E. 1969 Collective instability of salt fingers. *J. Fluid Mech.* **35**, 209–218.

Stokes, R. H. 1950 The diffusion coefficients of eight univalent electrolytes in aqueous sucrose solution at 25 °C. *J. Am. Chem. Soc.* **72**, 2243–2247.